Phase-amplitude coupling between mu- and gamma-waves to carry motor commands

Parth Chholak
Centro de Tecnología Biomédica
Universidad Politécnica de Madrid
Madrid, Spain
https://orcid.org/0000-0002-6437-7750

Alexander N. Pisarchik
Centro de Tecnología Biomédica
Universidad Politécnica de Madrid
Madrid, Spain
https://orcid.org/0000-0003-2471-2507

Semen A. Kurkin
Center for Technologies in Robotics and Mechatronics Components,
Innopolis University
Innopolis, Russia
https://orcid.org/0000-0002-3438-5717

Vladimir A. Maksimenko
Center for Technologies in Robotics and Mechatronics Components,
Innopolis University
Innopolis, Russia
https://orcid.org/0000-0002-4631-6896

Alexander E. Hramov
Center for Technologies in Robotics and Mechatronics Components,
Innopolis University
Innopolis, Russia
https://orcid.org/0000-0003-2787-2530

***Abstract*—The development of brain computer interfaces, especially the ones related to controlling exoskeletons and neurorehabilitation of stroke patients, strongly relies on our understanding of motor system and its neuronal mechanism. Motor imagery (MI) has turned out to be one of the most popular experimental regimes to study this system. Kinesthetic imagery (KI) is a kind of MI which shares a large portion of its neuronal pathway with real movements, except for having an additional inhibitory mechanism to prevent movement execution. Our magnetoencephalographic (MEG) experiments with ten untrained subjects revealed that this inhibitory control implied local neuronal desynchronization. We found that the motor-related communication between the inferior parietal cortex and the prefrontal cortex was carried out using the mu-frequency range. Additionally, three gamma frequencies were also pinpointed that encode the motor command specifics. Using artificial neural networks (ANNs) we classified left- and right-hand MI which reached maximal accuracy when we included these three gamma frequencies in the input signal for ANN. We suggest that mu-activity acts as a carrier of gamma-activity between inferior and parietal areas utilising phase-amplitude coupling.**

Keywords—brain-computer interface, motor imagery, inhibition, neuronal communication, phase-amplitude coupling, artificial neural network, magnetoencephalography (MEG)

I. Introduction

Brain-computer interfaces (BCIs) aim to control external devices using the operator's brain activity [1]. The BCI systems can be classified into two general categories [1]. In the first category, feedforward brain activity is used to control external devices and in the second category, a closed-loop feedback control is applied for neural rehabilitation.

The important task of BCIs is the pattern recognition of neurophysiological brain activity associated with motor imagery (MI) defined as a mental simulation of overt actions in the absence of any muscle movements. This bears crucial importance for brain-controlled exoskeletons, bioprosthesis and neurorehabilitation of amputee and post-stroke patients. The scientists distinguish two types of MI, visual imagery (VI) and kinesthetic imagery (KI) [2]. While in VI subjects MI activates visual cortex, in KI subjects the activity is detected in the same motor areas as in the case of real movements [2] with an additional mechanism for inhibiting motor commands to avoid overt actions [1], [3]–[5]. Functional magnetic resonance imaging (fMRI) studies evidence the involvement of motor associated areas and inferior parietal (IP) cortex for KI subjects, in contrast to VI subjects, who exhibit the involvement of visual and superior parietal cortices [6]. Moreover, transcranial magnetic stimulation (TMS) experiments suggest that the IP area participates in the inhibitory control of the primary motor cortex (M1) during KI-dominated MI [7]. However, despite extensive research on MI, no clear experimental evidence of the underlying KI mechanism has yet been provided.

One of the most popular experimental paradigms for MI studies is based on sensorimotor rhythms (SMR) [1], which involves KI of large body parts, such as whole limbs, to modulate neural activity [8]. At the same time, alpha- and beta-rhythms are crucial and ubiquitous in most studies on MI [9]. For example, in 1991 the alpha-rhythm was used to control the cursor position on a computer screen in one-dimensional space [10]. Later, more advanced and sophisticated methods, such as linear regression, logistic regression, and artificial neural networks (ANNs), were applied to control the cursor position in three-dimensional space [11]–[13], prosthetics [14]–[16], robots [17]–[21], and for stroke rehabilitation [16], [22], [23] (for review see [1], [24]).

Among a significant amount of literature on the BCI development using MI, electroencephalography (EEG) is found to be the most popular noninvasive technique [25]–[32] for controlling wheelchairs [25], communication aid systems [33], assistive and rehabilitative devices for healthy [34] and disabled people, stroke patients and people with other neurological deficits [26], [27], [35]–[37]. In addition, a fair amount of papers were devoted to magnetoencephalography (MEG) studies on MI [38]–[42], which has the advantage of a higher spatial resolution and better resilience against artifacts as compared to EEG, although some advantages of EEG, such as low cost and portability, are crucial for BCI development, but can be kept aside while understanding the fundamental activity underlying MI.

978-1-7281-2470-4/19/$31.00 ©2019 IEEE

The aim of this study is to analyse MEG signals, especially in alpha- and beta-frequency bands associated with MI in the SMR paradigm. We focus on the inhibitory mechanism to avoid overt action during KI, that was previously investigated using other neuroimaging techniques, such as TMS. Subsequently, we perform various validation tests along the way using methods based on the power spectrum anaslysis, coherence and ANNs, and suggest a model which explains empirical observations related to KI and real movements (overt actions).

II. Materials and Methods

The neurophysiological data were acquired using the Vectorview MEG system (Elekta AB) with 306 channels (102 magnetometers and 204 planar gradiometers) placed inside a magnetically shielded room (Vacuum Schmelze GmbH). Three fiducial points (nasion, left and right preauricular) were acquired for each subject.

The experimental study consisted of ten (nine right-handed, eight males) *untrained* volunteers between the age of 20 and 31. The subjects sat in a comfortable reclining chair with their legs straight, shoes off, and arms resting on an armrest in front of them. All of them provided a written informed-consent before the experiment commencement. The experimental studies were performed in accordance with the Declaration of Helsinki.

Spatiotemporal signal space separation [43] was used to separate neuronal signals from nearby electromagnetic interference. The signals from bad MEG channels were replaced with spatially-averaged signals of the nearby well-functioning MEG channels. The software used for this preprocessing task was MaxFilter that came along with the Elekta-Neuromag machine. The sampling frequency was 1000 Hz and an online anti-alias [0.1–330] Hz bandpass filter was utilised.

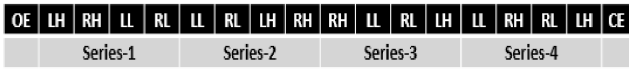

(a) Order of presentation.

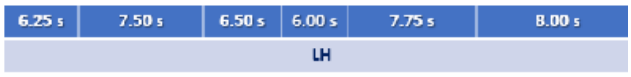

(b) MI trials for left hand.

The experimental protocol was designed as shown in Figure 1. Resting-state recordings were performed at the start and at the end of each experiment with open eyes (OE) and closed eyes (CE), respectively. OE recordings were later discarded because all data during MI were recorded with closed eyes. The duration of CE recordings was different for each subject and ranged from 40 to 280 s.

All MI recordings were divided into four sets of time series. Every set contained the MEG data of MI of each of four limbs in a random order, i.e., left hand (LH), right hand (RH), left leg (LL), and right leg (RL). The order of presentation shown in Figure 1(a) displays one of such protocols, which was different for each subject. Before MI of each limb, a visual message appeared on the screen to ask the subject close eyes and imagine the movement of the indicated limb as soon as a beep sounds. The subsequent beeps were given after a random time interval between 6 and 8 seconds. Each imaginary movement between the beeps was counted as one trial. Figure 1(b) shows a model example of the beep presentation for LH MI-trials. The number of trials for each limb was varied among subjects between 4 and 7 in each series. After every series, the subjects had a 40-s rest during which they listened to a relaxing music.

The experiments were programmed using software provided by the Cogent 2000 team at the Functional Imaging Laboratory and the Institute of Cognitive Neuroscience and Cogent Graphics developed by John Romaya at the Laboratory of Neurobiology at the Wellcome Department of Imaging Neuroscience. A MATLAB code was used to produce all audio and visual commands (Cogent) as well as to log the time at the beginning of each MI-trial in a protocol file (in .txt format). The protocol file was later used to mark all events manually when analysing the MEG file (in .fif format). A part of the data analysis was performed with Brainstorm [44] documented and freely available for downloading under the GNU general public license (http://neuroimage.usc.edu/brainstorm). Once the events were marked at the beginning of each limb's MI using the protocol file, 5-s trials were extracted immediately after these marks. Similarly, 10-s trials from CE-recordings were also marked and extracted as the background activity for every subject.

The time-frequency structure of the MEG signals was analysed using the wavelet approach, widely acceptable for the analysis of nonstationary biological and medical data [45]. For each limb, we used Morlet wavelets with $f_0 = 1$ Hz central frequency and a 3-s full width at half maximum (FWHM) to evaluate time-frequency spectrograms (TFSs) for all extracted 5-s MEG-trials of each limb, and then averaged the TFSs over all trials for that limb. Then, the TFS was also averaged over desired frequency ranges of delta (1–5 Hz) and mu (8–30 Hz). The same process was repeated for background 10-s trials using the same parameters. To evaluate ERS/ERD, we took the difference between the spectrogram for the MI-trials and the time-averaged spectrogram of the background and then normalized it to the background. This normalized difference was assumed to be positive for ERS and negative for ERD.

ANNs were used in the later stages for validation purposes. Multilayer perceptron (MLP) was chosen as the network architecture to classify between LH and RH MI-trials. The input data for the ANN were taken from MEG time series from all 102 magnetometers, after bandpass filtering with a 10-Hz passing window. This passing window was varied from 5-60 Hz in steps of 5 Hz, i.e., (5-15), (10-20), (15-25), ..., and (50-60) Hz. The input layer containing 102 neurons was followed by three hidden layers having 30, 15, and 5 neurons, respectively. The output layer consisted of a single neuron. Scaled conjugate gradient training algorithm was used. The training stopped as soon as the batch training with all input data ran for at least 5000 times. To improve the efficiency of machine learning, we randomly mixed the input signal maintaining the correspondence to the MI-type, either LH or RH. Therefore, to classify MI of LH and RH, we

mixed the MEG time series of all collected trials related to LH and RH for each channel without losing their corresponding targets (0 for LH and 1 for RH). The ANN classification was carried out using Neural Network Toolbox of MATLAB (R2017a; Mathworks Inc., MA, USA).

III. Results and Discussion

Based on differential mu-activity of the cortex, we first segregated the subjects into two groups, six KI subjects (Sub 1, 2, 4, 5, 9, and 10) and four VI subjects (Sub 3, 6, 7, and 8). The differentiation was performed according to ERD/ERS in the mu-frequency range. Specifically, the KI subjects exhibited ERD in the aforementioned associated cortical sites (

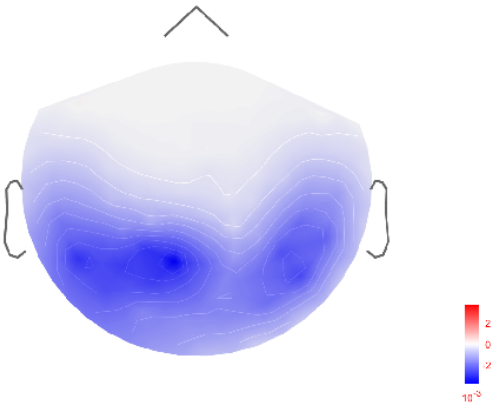

(a) ERS/ERD distribution for mu-frequency range averaged over all trails and trial time.

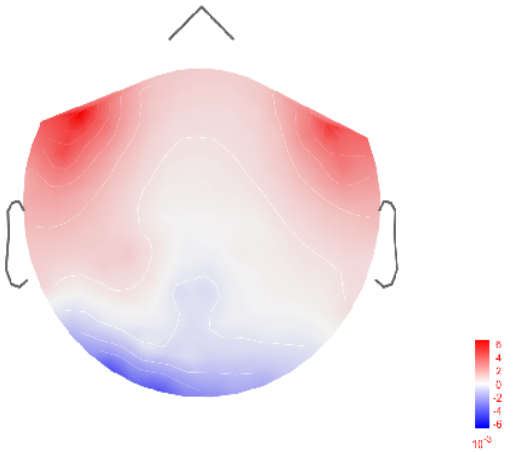

(b) ERS/ERD distribution for delta-frequency range averaged over all trails and trial time.

Figure 2: Event-related wavelet energy for subject-2 (KI).

Figure 2(a)), while the VI subjects showed ERS.

Curiously, the authors of [46] reported event-related desynchronisation (ERD) of mu-rhythms in the sensorimotor cortex during MI in the SMR paradigm and ERS for resting. Although the subjects in our study were instructed to perform KI, only some of them could successfully achieve this goal, because of the absent of preliminary traning.

The obtained results are in agreement with the previous study [46], where KI subjects (successful-SMR) exhibited ERD in mu-band, while VI subjects (failed-SMR) showed ERS, similar to the resting state of SMR. In the delta-range, all KI subjects exhibited either ERS or ERD in the prefrontal cortex (PF) and insignificant activty in the posterior parts of the brain (

Figure 2(b)). In addition, the VI subjects exhibited the distributed non-uniform activity without any preference for a particular region. The method used to evaluate ERS/ERD was as explained in section II.

As discussed in section I, KI and real movements share a common neuronal network, distinctly to KI which involves an additional mechanism for inhibiting overt movement that is likely to be situated in the IP. The coincidence of finding ERD for the KI subjects in mu-band at the same site as the one that is responsible for inhibitory control (i.e., IP) instils curiosity and deems to be further looked upon. In order to reveal the mechanism underlying this inhibitory control, we suppose that desynchronised activity of neurons near the IP disrupts signal propagation that passes from IP to M1, as hinted by TMS studies.

The PF is also known to be involved in inhibition of movements [47], more specifically in choosing between brain responses [48]. The authors of [49] showed that when subjects were asked to predict beforehand the time necessary to perform motor tasks, the subjects with lesions in the posterior parietal cortex typically underestimated/ overestimated the time. This strongly contrasted with subjects having dysfunctional motor regions, who exhibited impaired movements, but retained the ability to estimate motor performance times [50]. In order to predict motor performance times, the subject needs to simulate the entire repertoire of the act from long-term memory. This function is perhaps localised in the posterior parietal cortex. Conveniently, nearby temporal lobe has been implicated to play a role in long-term memory function, especially the medial temporal lobe [51].

Before the actual execution of motor commands by M1, aided by its associated areas like premotor cortex (PM) and supplementary motor area (SMA), passable responses are likely to be chosen at PF. As most of the conscious processing is performed in the frontal cortex, PF being the point hosting this decision-making process is amenable. We therefore propose the following neuronal pathway for motor signals (**Error! Reference source not found.**). Motor commands are generated in the posterior parietal cortex and need to travel to PF before being relayed to motor associated areas for final execution. ERD centred around IP disrupts the communication of motor commands from the posterior parietal cortex to PF in order to avoid any overt movement during KI.

The authors of [52] showed that bilateral lesions in the parietal cortex led to the execution of motor commands during MI experiments without the patient realising it. The patient with lesions at IP may not have ERD in IP at mu-frequency and would pass the signal to the PF region, not expecting an input from IP during KI and thus leading to actual execution without the subject's knowledge. We used coherence as a measure of connectivity between two parts of

the brain. The results indicate uninhibited communication in the mu-band between IP and PF for all VI subjects, whereas KI subjects exhibit a clearly compromised connectivity between these areas.

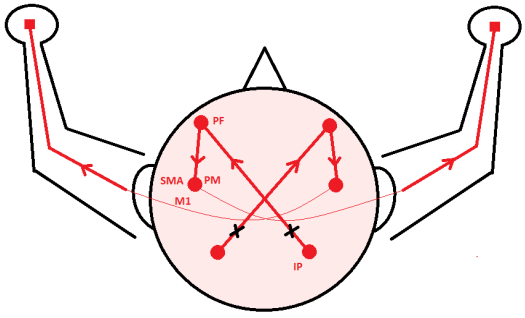

Figure 3: Neuronal pathway for KI. During KI, inhibition is manifested in the vicinity of IP in the form of ERD which prevents propagation of motor signal towards PF. The rest of the neural circuitry remains the same for MI and actual execution of motor commands

In Figure 4 we plot the mean-squared coherence of the MEG signals collected from IP and PF versus frequency (in Hz). The strength of connectivity between these areas was found to be suppressed for KI subjects as compared to the VI subjects and exhibit peaks at 10 (mu range), 32 (gamma range), 45 (gamma range), and 48 Hz (gamma range) for both groups of subjects.

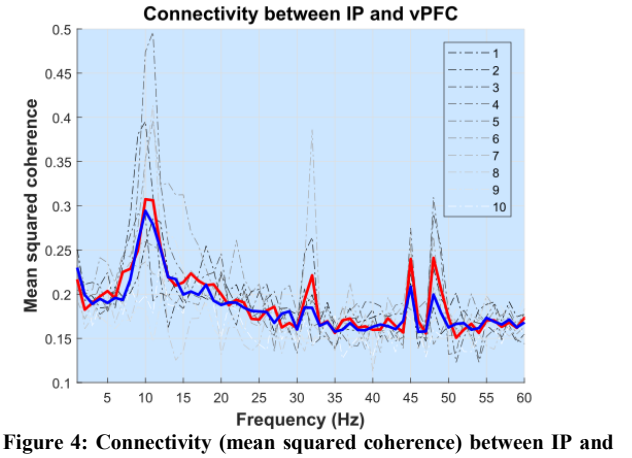

Figure 4: Connectivity (mean squared coherence) between IP and PF for all 10 subjects. Peaks obtained at 10 Hz (mu), 32 Hz (gamma), 45 Hz (gamma), and 48 Hz (gamma). The thick red and blue lines represent average connectivity of VI and KI subjects, respectively.

The authors of [53] discussed about a theta-gamma neural code for multi-message communication during memory processes. They prescribed phase-amplitude coupling between the phase of theta-waves and the amplitude of gamma-waves and envisaged upon the extension of their model to sensory processes if theta-waves are replaced by alpha-waves. The studies provide evidences of this phase-amplitude coupling in humans [54]–[[54]–[61].

During each gamma-cycle, a set of neurons or neural ensemble fire concurrently, forming a spatial pattern on the cortex that corresponds to the object being represented by that gamma-cycle. The authors of [62]–[65] showed that a sequence of generated information in the form of gamma-cycles gets mapped to different phases of theta-wave, maintaining the same order of information generation. Furthermore, the authors of [60] reported shifts in gamma phase-amplitude coupling frequency from theta to alpha during visual tasks. Similarly, we expect a phase-amplitude coupling between gamma and alpha/mu-waves for MI tasks.

We therefore suggest that motor commands involve mu-waves as general carriers of motor related activity. These carrier waves carry gamma-waves containing specifics of motor activity from IP to PF, which acts as a relay junction and transfers the information to motor related areas such as M1, PM, and SMA. The authors of [66]–[69] also evidence that the coherence in gamma-band between two points of the brain can be used to control neural communication between them.

Our ANN classification study designed in an unconventional but appropriate way, supports the hypothesis so far. The study was designed to find what frequency component of the MEG signal generates higher ANN accuracy in order to gauge the kind of ANN classification-task related information carried by that component.

As already mentioned in section II, the bandpass filtering in a 10-Hz window was used for preprocessing MEG data before the ANN classification of LH and RH MI. The classification accuracy was found to be independent of the type of MI. **Error! Reference source not found.** shows the ANN classification accuracy averaged over all subjects versus the bandpass frequency range. Each data point in this figure represents a centre of the corresponding bandpass frequency range. Thus, the points at the two local maxima represent 25–35 Hz and 45–55 Hz windows, respectively, as marked in **Error! Reference source not found.**. Observing these two maxima in the frequency ranges which include the gamma frequencies shown in `Figure 4` confirms our hypothesis that the MI specification (e.g., hand movement) is encoded in the gamma-wave. On the other hand, the mu-band played a general role in this motor task and did not contribute as much in differentiating two hands.

The amplitude of intracellular spiking in gamma-band in the directionality specific (LH or RH) neurons is codependent on the phase of the 10-Hz mu-band signal which acts as an envelope for motor-related activity between these regions.

In the very recent systematic and extensive review [9], only eight papers were mentioned in which authors employed MLP for deep neural network classification using EEG, and only three of which were focussed on MI. Only one of these MI studies utilised MEG time series as inputs for ANN [70] with a 75% accuracy, whereas other two studies [71], [72] used different forms of frequency transformations on the input signal and achieved up to 85% accuracy. The maximum accuracy obtained in our study, utilising MEG signals as input, was about 85% in the 40–50 Hz range.

IV. Conclusions

In this work we identified a neuronal pathway for motor command propagation during both kinesthetic imagery (KI) and real movements. We also revealed parts of the encoding details and signal disruption to avoid overt action. During KI, desynschronised neurons prevent brain activity in gamma (32, 45, and 48 Hz) carrying specifics of the movement to propagate from inferior parietal lobe to the prefrontal cortex which can blindly relay the signal to the motor areas for execution. All motor related communications are performed in the mu (10-Hz) frequency range using phase-amplitude coupling. Delta waves also participate in this circuit and definitely play an important role in the prefrontal cortex. We aspire that the identification of these motor related frequencies and the areas where they communicate through will turn out to be radical in developing BCIs henceforth [73], [74]. The insights about neural communication and inhibition may benefit research on controlling human inhibition towards harmful substances or preventing the propagation of undesirable sensations, such as pain.

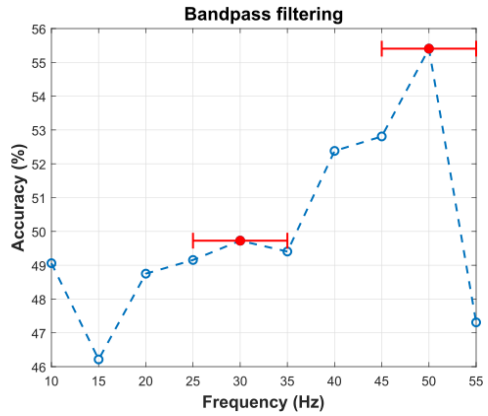

Figure 5: ANN accuracy in classification between LH and RH MI averaged over all subjects, versus bandpass frequency range on the input MEG signal to ANN. Each data point on the x-axis represents a central frequency of the 10-Hz bandpass frequency range.

Acknowledgment

This work was supported by the Spanish Ministry of Economy and Competitiveness (project SAF2016-80240) in the part of data acquisition and processing and by the President Program (projects NSH-2737.2018.2) and Russian Foundation for Basic Research (Project 16-29-08221) in the part of method development.

References

[1] R. Abiri, S. Borhani, E. W. Sellers, Y. Jiang, and X. Zhao, "A comprehensive review of EEG-based brain–computer interface paradigms," *J. Neural Eng.*, vol. 16, no. 1, p. 011001, Feb. 2019.

[2] P. Chholak *et al.*, "Visual and kinesthetic modes affect motor imagery classification in untrained subjects," *Sci. Reports 2019 91*, vol. 9, no. 1, p. 9838, Jul. 2019.

[3] A. Solodkin, P. Hlustik, E. E. Chen, and S. L. Small, "Fine Modulation in Network Activation during Motor Execution and Motor Imagery," *Cereb. Cortex*, vol. 14, no. 11, pp. 1246–1255, Nov. 2004.

[4] T. Hanakawa, M. A. Dimyan, and M. Hallett, "Motor Planning, Imagery, and Execution in the Distributed Motor Network: A Time-Course Study with Functional MRI," *Cereb. Cortex (New York, NY)*, vol. 18, no. 12, p. 2775, 2008.

[5] A. Guillot, F. Di Rienzo, T. Macintyre, A. Moran, and C. Collet, "Imagining is Not Doing but Involves Specific Motor Commands: A Review of Experimental Data Related to Motor Inhibition.," *Front. Hum. Neurosci.*, vol. 6, p. 247, 2012.

[6] A. Guillot, C. Collet, V. A. Nguyen, F. Malouin, C. Richards, and J. Doyon, "Brain activity during visual versus kinesthetic imagery: An fMRI study," *Hum. Brain Mapp.*, vol. 30, no. 7, pp. 2157–2172, Jul. 2009.

[7] F. Lebon, W. D. Byblow, C. Collet, A. Guillot, and C. M. Stinear, "The modulation of motor cortex excitability during motor imagery depends on imagery quality," *Eur. J. Neurosci.*, vol. 35, no. 2, pp. 323–331, Jan. 2012.

[8] V. Morash, O. Bai, S. Furlani, P. Lin, and M. Hallett, "Classifying EEG signals preceding right hand, left hand, tongue, and right foot movements and motor imageries," *Clin. Neurophysiol.*, vol. 119, no. 11, pp. 2570–2578, Nov. 2008.

[9] A. Craik, Y. He, and J. L. Contreras-Vidal, "Deep learning for electroencephalogram (EEG) classification tasks: a review," *J. Neural Eng.*, vol. 16, no. 3, p. 031001, Jun. 2019.

[10] J. R. Wolpaw, D. J. McFarland, G. W. Neat, and C. A. Forneris, "An EEG-based brain-computer interface for cursor control," *Electroencephalogr. Clin. Neurophysiol.*, vol. 78, no. 3, pp. 252–259, Mar. 1991.

[11] J. R. Wolpaw and D. J. McFarland, "Control of a two-dimensional movement signal by a noninvasive brain-computer interface in humans," *Proc. Natl. Acad. Sci.*, vol. 101, no. 51, pp. 17849–17854, Dec. 2004.

[12] J. R. Wolpaw and D. J. McFarland, "Multichannel EEG-based brain-computer communication," *Electroencephalogr. Clin. Neurophysiol.*, vol. 90, no. 6, pp. 444–449, Jun. 1994.

[13] D. J. McFarland, W. A. Sarnacki, and J. R. Wolpaw, "Electroencephalographic (EEG) control of three-dimensional movement," *J. Neural Eng.*, vol. 7, no. 3, p. 036007, Jun. 2010.

[14] A. R. Murguialday *et al.*, "Brain-Computer Interface for a Prosthetic Hand Using Local Machine Control and Haptic Feedback," in *2007 IEEE 10th International Conference on Rehabilitation Robotics*, 2007, pp. 609–613.

[15] C.-W. Chen, C.-C. K. Lin, and S. J Ming, "Hand Orthosis Controlled Using Brain-computer Interface," *J Med Biol Eng*, vol. 29, pp. 234–241, 2008.

[16] A. Ramos-Murguialday *et al.*, "Brain-Machine-Interface in Chronic Stroke Rehabilitation: A Controlled Study," *Ann. Neurol.*, vol. 74, no. 1, p. 100, 2013.

[17] G. R. Müller-Putz, R. Scherer, G. Pfurtscheller, and R. Rupp, "EEG-based neuroprosthesis control: A step towards clinical practice," *Neurosci. Lett.*, vol. 382, no. 1–2, pp. 169–174, Jul. 2005.

[18] Kai Keng Ang *et al.*, "A clinical study of motor imagery-based brain-computer interface for upper limb robotic rehabilitation," in *2009 Annual International Conference of the IEEE Engineering in Medicine and Biology Society*, 2009, pp. 5981–5984.

[19] M. Sarac, E. Koyas, A. Erdogan, M. Cetin, and V. Patoglu, "Brain Computer Interface based robotic rehabilitation with online modification of task speed," in *2013 IEEE 13th International Conference on Rehabilitation Robotics (ICORR)*, 2013, pp. 1–7.

[20] B. S. Baxter, A. Decker, and B. He, "Noninvasive control of a robotic arm in multiple dimensions using scalp electroencephalogram," in *2013 6th International IEEE/EMBS Conference on Neural Engineering (NER)*, 2013, pp. 45–47.

[21] K. LaFleur, K. Cassady, A. Doud, K. Shades, E. Rogin, and B. He, "Quadcopter control in three-dimensional space using a noninvasive motor imagery-based brain-computer interface.," *J. Neural Eng.*, vol. 10, no. 4, p. 046003, Aug. 2013.

[22] T. Ono *et al.*, "Brain-computer interface with somatosensory feedback improves functional recovery from severe hemiplegia due to chronic stroke," *Front. Neuroeng.*, vol. 7, p. 19, Jul. 2014.

[23] S. M. Rayegani *et al.*, "Effect of Neurofeedback and Electromyographic-Biofeedback Therapy on Improving Hand Function in Stroke Patients," *Top. Stroke Rehabil.*, vol. 21, no. 2, pp. 137–151, Mar. 2014.

[24] K. K. Ang and C. Guan, "EEG-Based Strategies to Detect Motor Imagery for Control and Rehabilitation," *IEEE Trans. Neural Syst. Rehabil. Eng.*, vol. 25, no. 4, pp. 392–401, Apr. 2017.

[25] L. Bi, X.-A. Fan, and Y. Liu, "EEG-Based Brain-Controlled Mobile Robots: A Survey," *IEEE Trans. Human-Machine Syst.*, vol. 43, no. 2, pp. 161–176, Mar. 2013.

[26] S. Machado, L. F. Almada, and R. N. Annavarapu, "Progress and Prospects in EEG-Based Brain-Computer Interface: Clinical Applications in Neurorehabilitation," *J. Rehabil. Robot.*, vol. 1,

no. 1, pp. 28–41, Jun. 2013.
[27] S. Moghimi, A. Kushki, A. Marie Guerguerian, and T. Chau, "A Review of EEG-Based Brain-Computer Interfaces as Access Pathways for Individuals with Severe Disabilities," *Assist. Technol.*, vol. 25, no. 2, pp. 99–110, Apr. 2013.
[28] T. M. Vaughan, J. R. Wolpaw, and E. Donchin, "EEG-based communication: prospects and problems," *IEEE Trans. Rehabil. Eng.*, vol. 4, no. 4, pp. 425–430, 1996.
[29] H.-J. Hwang, S. Kim, S. Choi, and C.-H. Im, "EEG-Based Brain-Computer Interfaces: A Thorough Literature Survey," *Int. J. Hum. Comput. Interact.*, vol. 29, no. 12, pp. 814–826, Dec. 2013.
[30] F. Lotte, M. Congedo, A. Lécuyer, F. Lamarche, and B. Arnaldi, "A review of classification algorithms for EEG-based brain–computer interfaces," *J. Neural Eng.*, vol. 4, no. 2, pp. R1–R13, Jun. 2007.
[31] "Encyclopedia of Biomedical Engineering," 1st ed., vol. 2, New Jersey: John Wiley and Sons, 2006, pp. 1156–1166.
[32] S. Machado *et al.*, "EEG-based brain-computer interfaces: an overview of basic concepts and clinical applications in neurorehabilitation.," *Rev. Neurosci.*, vol. 21, no. 6, pp. 451–68, 2010.
[33] N. Birbaumer *et al.*, "A spelling device for the paralysed," *Nature*, vol. 398, no. 6725, pp. 297–298, Mar. 1999.
[34] J. Meng, S. Zhang, A. Bekyo, J. Olsoe, B. Baxter, and B. He, "Noninvasive Electroencephalogram Based Control of a Robotic Arm for Reach and Grasp Tasks," *Sci. Rep.*, vol. 6, no. 1, p. 38565, Dec. 2016.
[35] J. J. Daly and J. R. Wolpaw, "Brain–computer interfaces in neurological rehabilitation," *Lancet Neurol.*, vol. 7, no. 11, pp. 1032–1043, Nov. 2008.
[36] N. Birbaumer and L. G. Cohen, "Brain-computer interfaces: communication and restoration of movement in paralysis," *J. Physiol.*, vol. 579, no. 3, pp. 621–636, Mar. 2007.
[37] N. Birbaumer, "Breaking the silence: Brain?computer interfaces (BCI) for communication and motor control," *Psychophysiology*, vol. 43, no. 6, pp. 517–532, Nov. 2006.
[38] R. Salmelin and R. Hari, "Spatiotemporal characteristics of sensorimotor neuromagnetic rhythms related to thumb movement," *Neuroscience*, vol. 60, no. 2, pp. 537–550, May 1994.
[39] A. Schnitzler, S. Salenius, R. Salmelin, V. Jousmäki, and R. Hari, "Involvement of Primary Motor Cortex in Motor Imagery: A Neuromagnetic Study," *Neuroimage*, vol. 6, no. 3, pp. 201–208, Oct. 1997.
[40] L. Kauhanen, P. Rantanen, J. A. Lehtonen, I. Tarnanen, H. Alaranta, and M. Sams, "'Sensorimotor cortical activity of tetraplegics during attempted finger movements' intention and imagery," *Biomed. Tech.*, vol. 49, pp. 59–60, 2004.
[41] H.-L. Halme and L. Parkkonen, "Comparing Features for Classification of MEG Responses to Motor Imagery," *PLoS One*, vol. 11, no. 12, p. e0168766, 2016.
[42] H.-L. Halme and L. Parkkonen, "Across-subject offline decoding of motor imagery from MEG and EEG," *Sci. Rep.*, vol. 8, no. 1, p. 10087, Dec. 2018.
[43] S. Taulu and R. Hari, "Removal of magnetoencephalographic artifacts with temporal signal-space separation: Demonstration with single-trial auditory-evoked responses," *Hum. Brain Mapp.*, vol. 30, no. 5, pp. 1524–1534, May 2009.
[44] F. F. Tadel, S. Baillet, J. C. Mosher, D. Pantazis, and R. M. Leahy, "Brainstorm: A user-friendly application for MEG/EEG analysis," *Comput. Intell. Neurosci.*, vol. 2011, p. 879716, Apr. 2011.
[45] P. C. Ivanov, A. L. Goldberger, S. Havlin, C.-K. Peng, M. G. Rosenblum, and H. E. Stanley, "Wavelets in medicine and physiology," in *Wavelets in Physics*, J. C. van den Berg, Ed. Cambridge: Cambridge University Press, 1999, pp. 391–420.
[46] G. Pfurtscheller and F. H. Lopes da Silva, "Event-related EEG/MEG synchronization and desynchronization: basic principles," *Clin. Neurophysiol.*, vol. 110, no. 11, pp. 1842–1857, Nov. 1999.
[47] M. Krams, M. F. S. Rushworth, M.-P. Deiber, R. S. J. Frackowiak, and R. E. Passingham, "The preparation, execution and suppression of copied movements in the human brain," *Exp. Brain Res.*, vol. 120, no. 3, pp. 386–398, May 1998.
[48] J. Duque, L. Labruna, S. Verset, E. Olivier, and R. B. Ivry, "Dissociating the role of prefrontal and premotor cortices in controlling inhibitory mechanisms during motor preparation.," *J. Neurosci.*, vol. 32, no. 3, pp. 806–16, Jan. 2012.
[49] A. Sirigu, J. R. Duhamel, L. Cohen, B. Pillon, B. Dubois, and Y. Agid, "The mental representation of hand movements after parietal cortex damage," *Science (80-.).*, vol. 273, pp. 1564–1568, 1996.
[50] A. Sirigu *et al.*, "Congruent unilateral impairments for real and imagined hand movements," *Neuroreport*, vol. 6, pp. 997–1001, 1995.
[51] A. Jeneson and L. R. Squire, "Working memory, long-term memory, and medial temporal lobe function.," *Learn. Mem.*, vol. 19, no. 1, pp. 15–25, Jan. 2012.
[52] J. Schwoebel, C. B. Boronat, and H. Branch Coslett, "The man who executed ``imagined" movements: evidence for dissociable components of the body schema," *Brain Cogn.*, vol. 50, pp. 1–16, 2002.
[53] J. E. Lisman and O. Jensen, "The θ-γ neural code.," *Neuron*, vol. 77, no. 6, pp. 1002–16, Mar. 2013.
[54] R. Llinás and U. Ribary, "Coherent 40-Hz oscillation characterizes dream state in humans.," *Proc. Natl. Acad. Sci. U. S. A.*, vol. 90, no. 5, pp. 2078–81, Mar. 1993.
[55] F. Mormann *et al.*, "Phase/amplitude reset and theta-gamma interaction in the human medial temporal lobe during a continuous word recognition memory task," *Hippocampus*, vol. 15, no. 7, pp. 890–900, Jan. 2005.
[56] R. T. Canolty *et al.*, "High gamma power is phase-locked to theta oscillations in human neocortex.," *Science*, vol. 313, no. 5793, pp. 1626–8, Sep. 2006.
[57] T. Demiralp *et al.*, "Gamma amplitudes are coupled to theta phase in human EEG during visual perception," *Int. J. Psychophysiol.*, vol. 64, no. 1, pp. 24–30, Apr. 2007.
[58] P. Sauseng *et al.*, "Brain Oscillatory Substrates of Visual Short-Term Memory Capacity," *Curr. Biol.*, vol. 19, no. 21, pp. 1846–1852, Nov. 2009.
[59] N. Axmacher, M. M. Henseler, O. Jensen, I. Weinreich, C. E. Elger, and J. Fell, "Cross-frequency coupling supports multi-item working memory in the human hippocampus.," *Proc. Natl. Acad. Sci. U. S. A.*, vol. 107, no. 7, pp. 3228–33, Feb. 2010.
[60] B. Voytek, R. T. Canolty, A. Shestyuk, N. E. Crone, J. Parvizi, and R. T. Knight, "Shifts in Gamma Phase–Amplitude Coupling Frequency from Theta to Alpha Over Posterior Cortex During Visual Tasks," *Front. Hum. Neurosci.*, vol. 4, 2010.
[61] E. Maris, M. van Vugt, and M. Kahana, "Spatially distributed patterns of oscillatory coupling between high-frequency amplitudes and low-frequency phases in human iEEG.," *Neuroimage*, vol. 54, no. 2, pp. 836–50, Jan. 2011.
[62] W. E. Skaggs, B. L. McNaughton, M. A. Wilson, and C. A. Barnes, "Theta phase precession in hippocampal neuronal populations and the compression of temporal sequences," *Hippocampus*, vol. 6, no. 2, pp. 149–172, Jan. 1996.
[63] K. D. Harris, J. Csicsvari, H. Hirase, G. Dragoi, and G. Buzsáki, "Organization of cell assemblies in the hippocampus," *Nature*, vol. 424, no. 6948, pp. 552–556, Jul. 2003.
[64] G. Dragoi and G. Buzsáki, "Temporal Encoding of Place Sequences by Hippocampal Cell Assemblies," *Neuron*, vol. 50, no. 1, pp. 145–157, Apr. 2006.
[65] A. S. Gupta, M. A. A. van der Meer, D. S. Touretzky, and A. D. Redish, "Segmentation of spatial experience by hippocampal θ sequences.," *Nat. Neurosci.*, vol. 15, no. 7, pp. 1032–9, Jun. 2012.
[66] S. L. Bressler, "Large-scale cortical networks and cognition," *Brain Res. Rev.*, vol. 20, no. 3, pp. 288–304, Mar. 1995.
[67] F. Varela, J.-P. Lachaux, E. Rodriguez, and J. Martinerie, "The brainweb: Phase synchronization and large-scale integration," *Nat. Rev. Neurosci.*, vol. 2, no. 4, pp. 229–239, Apr. 2001.
[68] P. Fries, "A mechanism for cognitive dynamics: neuronal communication through neuronal coherence," *Trends Cogn. Sci.*, vol. 9, no. 10, pp. 474–480, Oct. 2005.
[69] M. Siegel, T. H. Donner, and A. K. Engel, "Spectral fingerprints of large-scale neuronal interactions," *Nat. Rev. Neurosci.*, vol. 13, no. 2, pp. 121–134, Feb. 2012.
[70] I. Sturm, S. Lapuschkin, W. Samek, and K.-R. Müller, "Interpretable deep neural networks for single-trial EEG classification," *J. Neurosci. Methods*, vol. 274, pp. 141–145, Dec. 2016.
[71] S. A. C. Yohanandan, I. Kiral-Kornek, J. Tang, B. S. Mshford, U. Asif, and S. Harrer, "A Robust Low-Cost EEG Motor Imagery-Based Brain-Computer Interface," in *2018 40th Annual*

International Conference of the IEEE Engineering in Medicine and Biology Society (EMBC), 2018, pp. 5089–5092.

[72] Q. She, B. Hu, Z. Luo, T. Nguyen, and Y. Zhang, "A hierarchical semi-supervised extreme learning machine method for EEG recognition," *Med. Biol. Eng. Comput.*, vol. 57, no. 1, pp. 147–157, Jan. 2019.

[73] M. M. Danziger, O. I. Moskalenko, S. A. Kurkin, X. Zhang, S. Havlin, S. Boccaletti, "Explosive synchronization coexists with classical synchronization in the Kuramoto model," Chaos: An Interdisciplinary Journal of Nonlinear Science, V. 26, no. 6, p.065307, 2016.

[74] V. A. Maksimenko, S. A. Kurkin, E. N. Pitsik, V. Y. Musatov, A. E. Runnova, T. Y. Efremova, A. E. Hramov, A. N. Pisarchik, "Artificial neural network classification of motor-related eeg: An increase in classification accuracy by reducing signal complexity," Complexity, V. 2018, no. 9385947, 2018